High-resolution photoneutron study of $E1$ and $M1$ transitions in ^{208}Pb

R. J. Holt, H. E. Jackson, R. M. Laszewski,* and J. R. Specht
Argonne National Laboratory, Argonne, Illinois 60439
(Received 29 December 1978)

The photoneutron cross section of ^{208}Pb was observed using a very high resolution time-of-flight spectrometer. The cross sections were observed in the photoneutron energy range 16 to 1000 keV and at reaction angles of 90° and 135°. The deduced ground-state radiative widths were calibrated to the well-known ^{2}H(γ,n)^{1}H reaction cross section. The 7.99-MeV resonance, previously believed to be an $M1$ excitation, is shown to be an $E1$ resonance. Current progress in the search for the collective $M1$ resonance in ^{208}Pb is reviewed. In addition, recent theoretical predictions of the properties of the giant $M1$ resonance are reviewed. Finally, the present high resolution observations in conjunction with previous photoneutron polarization measurements were employed in order to deduce the s-d-wave admixtures for eight $E1$ excitations.

[NUCLEAR REACTIONS ^{208}Pb(γ,n)^{207}Pb, E_{exc} = 7.4–8.4 MeV, observed $\sigma(\theta)$, θ = 90°, 135°; deduced $\Gamma_{\gamma 0}$, J^{π}.]

I. INTRODUCTION

Interest in the search for non-$E1$ collective resonances has been intense during the past decade. The prospect of giant magnetic dipole resonances in heavy nuclei, particularly ^{208}Pb, has spurred numerous theoretical and experimental studies. The problem of $M1$ excitations in ^{208}Pb has been intriguing, since one would expect an ideal demonstration of a giant magnetic dipole resonance (GMDR) in this nucleus. For example, both the proton ($h_{11/2} \rightarrow h_{9/2}$) and neutron ($i_{13/2} \rightarrow i_{11/2}$) spin-flip transitions can contribute to the GMDR. Interest in the possibility of a GMDR in ^{208}Pb began when Bowman *et al.*[1] reported evidence for enhanced $M1$ strength in photoneutron studies of ^{208}Pb. What followed was a series of extremely difficult, but elegant experiments[2-21] and an intense development[22-28] of theory which has culminated in a new concept[28] in the schematic particle-hole theory of giant resonances. This new theoretical development[28] allows one to explain, for the first time, the correct centroid of the giant electric dipole resonance in ^{208}Pb.

Although the experimental and theoretical developments will be briefly summarized here, the present work will focus on the high-resolution, both polarized and unpolarized photoneutron experiments performed at the Argonne high-current electron accelerator facility during the past three years. The threshold photoneutron polarization studies[6,7] demonstrated that most of the $M1$ strength observed in Ref. 1 was, indeed, $E1$ in nature. However, the photoneutron polarization method indicated that there was a strong $M1$ excitation at 7.99 MeV, in agreement with Refs. 1 and 5. The photoneutron polarization results are reviewed in Sec. III. In order to study this excitation region in detail, we observed the ^{208}Pb(γ, n_0)/^{207}Pb reaction with extremely high resolution using the unique 35-ps wide electron-pulse mode and the newly installed 25-m neutron flight paths at the Argonne linac facility. The objectives of this high-resolution study were (1) to resolve fine structure, particularly in the vicinity of the 7.99-MeV (E_n = 610-keV) resonance, (2) to provide values of ground-state radiation widths which were calibrated to the well-known ^{2}H(γ, n)^{1}H reaction cross section, and (3) to provide accurate photoneutron angular-distribution information. It is shown in Sec. II from the new high-resolution data that the 7.99-MeV resonance is unequivocally an $E1$ excitation. Another important finding is that the ground-state radiation widths for the resonances in this region are approximately half of the previously believed values.[3]

The values of s-d-wave admixtures were determined for eight $E1$ excitations below E_n = 1.0 MeV. Despite the suppression by the penetrability effect, the d-wave components of the neutron decay widths were found to be larger than the s-wave widths for four of the levels. Harvey and Khanna[29] used a schematic model for describing 1^- excitations in ^{208}Pb. They predicted that the ratios of d-to-s amplitudes for $E1$ resonances were large throughout the energy range encompassed by the present observations. The question of large d-wave admixtures is discussed in Sec. V A.

II. HIGH-RESOLUTION STUDY OF ^{208}Pb

A. Experimental method

The key component of the Argonne threshold photoneutron facility is the unique high-current electron accelerator. The linac can be operated in a mode[30] (pico pulse mode) that produces electron bursts of 35-ps duration and 200-A peak current at a rate of 800 Hz. This pico pulse mode enables precise, high-resolution photoneutron studies of nuclei. The unique pico pulse mode used in conjunction with the newly installed 25-m flight paths allows an energy resolution previously unattained in photoneutron physics studies. The importance of high-resolution photoneutron experiments will be demonstrated for the ^{208}Pb nucleus in Sec. II B. In the present experiment 8.5-MeV electrons were extracted from the Argonne high-current linac while it was operating in the pico pulse mode. The energy-analyzed electron beam was focused onto an Ag foil (1.5 mm thick). The bremsstrahlung photons from this process then irradiated a thin slab (2.5 cm×5.0 cm×0.3 cm) of enriched (99.1%) ^{208}Pb metal. The remaining electrons were stopped in a 2.5-cm-thick Al block located immediately behind the converter. The current signal from the stopped electrons provides a "start" pulse for the time-of-flight spectrometer. The photoneutrons then travel through two 25-m flight paths which are at angles of 90° and 135° with respect to the electron beam axis. The neutron beam was filtered through 2.0-cm-thick Bi plates located approximately 1 m along each flight path. These Bi filters suppressed low energy γ rays which were created in the bremsstrahlung process and scattered from the sample. Finally, the neutrons were detected at the end of each flight path in a 5.0 cm×20.0 cm×1.0 cm (2.5 cm at 90°) thick NE110 plastic scintillator which was optically coupled to two RCA 8575 photomultipliers. The signals from each photomultiplier triggered a constant fraction discriminator (ORTEC, model 473). The outputs of the discriminators were taken in coincidence in order to define a neutron event. The output pulse from the first coincidence circuit (ORTEC, model C134) provided a "stop" trigger for the time digitizer (EG and G, model TDC100). The overall time resolution was found to be ~1.4 ns by directly observing the γ flash produced in the bremsstrahlung converter. The energy resolution of the time-of-flight spectrometer ranged between 0.2 keV at 180 keV and 1.5 keV at 1000 keV.

The raw time-of-flight data for this experiment are shown in Fig. 1. These spectra were recorded in 0.5-ns time bins. The two upper panels in the figure show the spectra recorded at 90°, while the lower panels show the data at 135°. The photoneutron energies are given in units of keV. The lines connecting the data points were drawn as a guide to the eye. The data not only exemplify the high resolution of the spectrometer, but also demonstrate the excellent signal-to-background ratio that can be achieved with a high-current electron linac. The inset figures show the 600-keV region in ^{208}Pb in detail. The 610-keV resonance was previously believed to be an $M1$ excitation. These data clearly show a constructive interference effect between the 600- and 610-keV resonances indicating that both resonances have the same spin and parity. This problem will be discussed in detail in Sec. II B.

The ground-state radiative widths were calibrated to the well-known ^{2}H(γ, n)^{1}H cross section in the following manner. With the accelerator operating in the same conditions as described above, the ^{208}Pb sample was replaced with a 5.0-mm-thick (other dimensions are the same as those of the ^{208}Pb sample) CD_2 sample. At a given γ-ray energy the cross section for the ^{208}Pb(γ, n_0)^{207}Pb reaction was determined from the cross section for the ^{2}H(γ, n)^{1}H reaction. The deuteron photodisintegration cross section was computed from the well-known n-p total capture cross section[31] and the predicted electric and magnetic components[32] of the photodisintegration process.

In order to determine the shapes of the detector efficiency curves, the electron energy was increased to 10.0 MeV and a 1.0-mm-thick C^2H_2 target was placed in the photon beam. The increased electron energy eliminates the problems associated with knowing the bremsstrahlung shape near the end-point energy. The use of the thin C^2H_2 sample minimizes the effects of neutron multiple scattering events in the target. Multiple scattering effects were found to be large (~20%) for a 5.0-mm-thick C^2H_2 target below a neutron energy of 500 keV.

The region below 300 keV was studied in the following manner. The electron end-point energy was reduced to 8.2 MeV in order to eliminate the effects on non-ground-state neutron transitions. Neutron detectors which consisted of ^{6}Li-loaded glass were placed at flight path lengths of 10.0 m and the electron burst width was tuned to 4 ns in duration. The detector efficiency shapes were determined from the well-known cross section for the ^{6}Li(n, α)^{3}H reaction. The ground-state radiative widths were calibrated to that of the 314-keV resonance, which was determined in the high-resolution study. The raw time-of-flight data for the 30–300 keV region are shown in Fig. 2. Again, the spectra at both 90° and 135° are shown. The large signal-to-background ratio eases the deter-

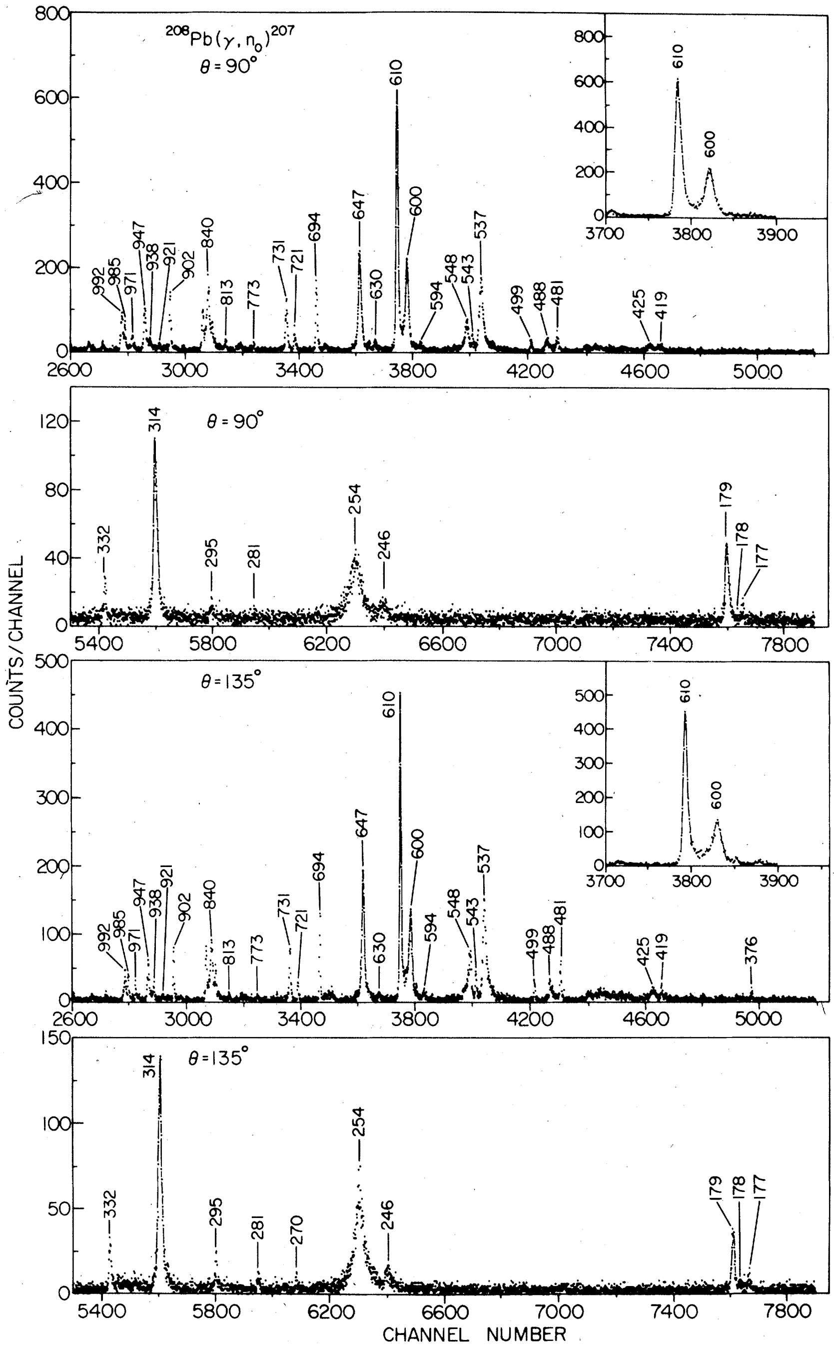

FIG. 1. Very high-resolution, raw time-of-flight spectra for the $^{208}Pb(\gamma, n_0)^{207}Pb$ reaction. The inset figures show the region of the 610-keV resonance, a suspected $M1$ excitation, in detail. The photoneutron energies are given in keV.

mination of accurate ground-state radiative widths. The broad apparent peak in the spectra at approximately 250 keV is due to the 250-keV resonance in the $^{6}Li(n, \alpha)\,^{3}H$ reaction.

B. Results of the high-resolution experiment

Perhaps the most interesting aspect of these high-resolution data is the 600-, 610-keV reso-

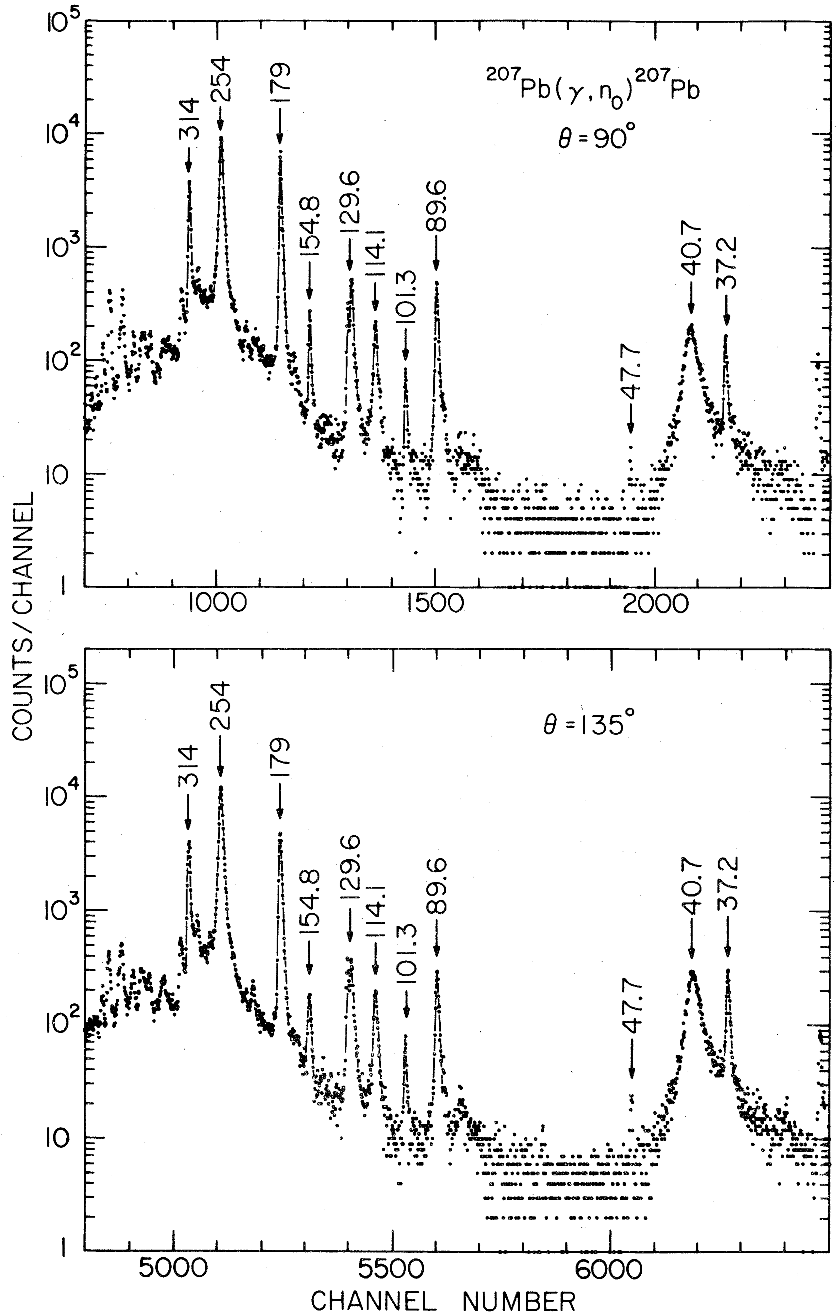

FIG. 2. Time-of-flight spectra for the ^{208}Pb(γ,n_0)^{207}Pb in the energy region 30–330 keV.

nance region. From the inset figures in Fig. 1, one can readily see that there is a constructive interference pattern between these two resonances. It is now known that previous photoneutron polarization data[6] falsely indicated that the 610-keV resonance was an $M1$ excitation. The photoneutron polarization method will be discussed in Sec. III and this problem will be addressed there. The 610-keV resonance was the only remaining large excitation that was previously believed to be an $M1$ resonance. We show here that this resonance is $E1$ in nature and, consequently, that no large single $M1$ excitations have thus far been observed in ^{208}Pb. The photoneutron polarization data[6] have shown that the 600-keV resonance is an $E1$ excitation. This has been confirmed by the results of

Horen *et al.*[11] The constructive interference pattern is due to level-level interference in which both the 600- and 610-keV resonances have the same spin and parity, 1^-. This can be seen clearly from Fig. 3. Here the observed cross sections at angles of 90° and 135° are shown in detail along with two multilevel analyses of the data. Clearly, the case where both levels are $E1$ describes the data much better than an $E1$ level at 600 keV and an $M1$ at 610 keV. In particular, the $E1$-$M1$ resonance combination fails to describe the valley between the levels. The parameters which were used in the $E1$-$E1$ analysis are given in Table I. In the analysis a small $E2$ resonance ($\Gamma_{\gamma 0}=0.4$ eV) was

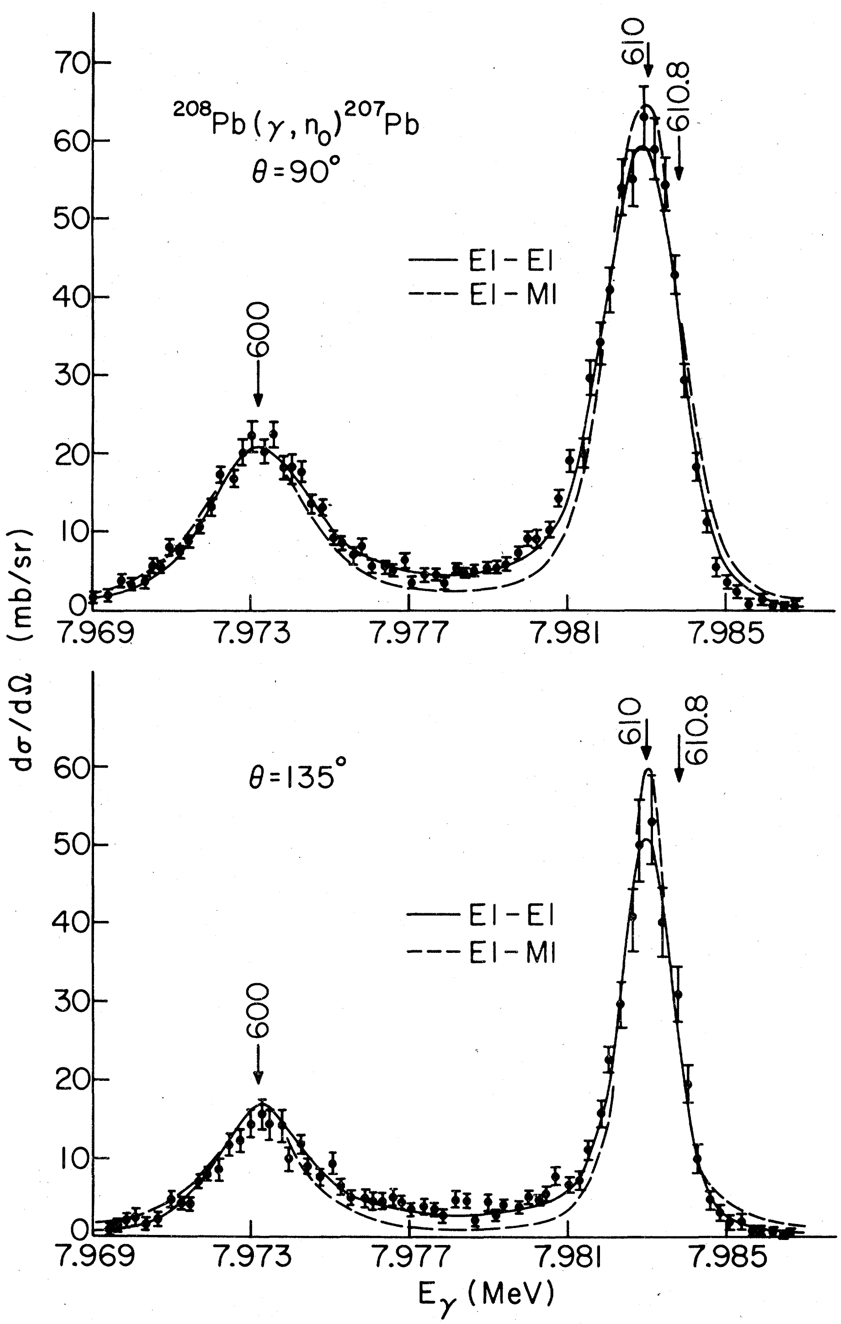

FIG. 3. Cross sections for the ^{208}Pb(γ,n_0)^{207}Pb reaction at 90° and 135° and in the vicinity of the 600- and 610-keV resonances. The solid curve represents the multilevel analysis when the two resonances are $E1$ excitations, while the dashed curve is the result when the 610-keV resonance is assumed to be an $M1$ excitation.

TABLE I. R-matrix parameters for the analysis of the 600-keV region in the $^{208}Pb(\gamma, n_0)^{207}Pb$ reaction.

E_γ (MeV)	$m\mathcal{L}$	$\Gamma_{\gamma 0}$ (eV)	l_1	Γ_{n1} (keV)	l_2	Γ_{n2} (keV)
7.9731	$E1$	5.5	0	0.20	2	2.2
7.9828	$E1$	8.9	0	0.04	2	0.785
7.9838	$E2$	0.4	1	0.14	3	0.03

placed at 610.8 keV in agreement with a resonance seen in neutron scattering[11] and neutron capture[33] data. The inclusion of a non-$E1$ resonance here allows the observed angular-distribution ratio $R = 1.57$ to be described. Without another level here the maximum angular-distribution ratio would be 1.42 with the choices of nonresonant phases given in Table I. A small non-$E1$ resonance here also explains the nonzero photoneutron polarization observed at 90°, as pointed out in Ref. 11. It is clear that more than a 3-level analysis would be necessary to fully describe the (γ, n) polarization at 90° in this energy region. Since only the two large levels can be directly observed, it is difficult, if not impossible, to know the correct reaction mechanism for the small, hidden levels. Consequently, no attempt was made to describe the polarization at 90°. However, the polarization at 135° is dominated by the s-d-wave admixture of the two large $E1$ resonances. Thus, the polarization was predicted from the parameters (Table I) that describe the high-resolution data (see Fig. 4). The predicted polarization at 135° is in reasonable agreement with the observed polarization.

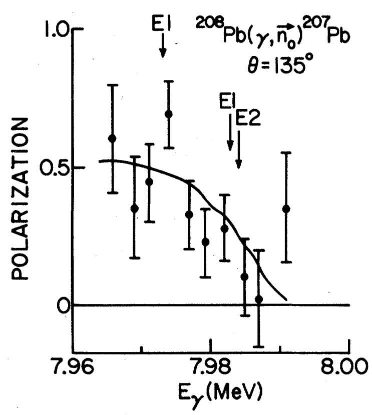

FIG. 4. Photoneutron polarization for the $^{208}Pb(\gamma, n_0)^{207}Pb$ reaction at 135°. The curve is the prediction based upon the R-matrix analysis of the high-resolution (γ, n) cross sections. In the analysis, it was assumed that the two major levels in this region are $E1$ excitation. The arrows indicate the locations of the resonances in this analysis.

The deduced ground-state radiative widths and angular-distribution ratios $R \equiv \sigma(90°)/\sigma(135°)$ for the $^{208}Pb(\gamma, n_0)^{207}Pb$ reaction are given in Table II. The results here depart from previous (γ, n) (Refs. 1–3 and 5) or (n, γ) (Ref. 10) observations in that the $\Gamma_{\gamma 0}$ and angular distributions in the present measurement were calibrated to the well-known $^2H(\gamma, n)^1H$ cross section. The observed $\Gamma_{\gamma 0}$ here is approximately two times smaller than those of Ref. 3. This was evidently due to a large multiple neutron scattering effect on the detector efficiency curve near 254 keV, the energy of the calibration resonance of Ref. 3, from the thick ^2H_2O sample used. The present work circumvents these problems by utilizing a very thin C^2H_2 sample.

A comparison of the present high-resolution work with the photoneutron results of Bowman *et al.*[1] and Haacke and McNeill[5] is given in Table III. Although these three photoneutron measurements are independent, the work of both Refs. 1 and 5 was calibrated to the $\Gamma_{\gamma 0}$ of the 40.7-keV resonance. The $\Gamma_{\gamma 0}$ of this resonance was thought to be known ($\Gamma_{\gamma 0} = 4.2$ eV) from (n, γ) experiments.[34] However, it appears that this is a difficult measurement for the (n, γ) method. In fact, in more recent neutron capture work[10] the 40.7-keV resonance was reported to have $\Gamma_{\gamma 0} = 5.1$ eV. This would tend to increase the Livermore and Toronto ground-state radiative widths. The present work is independent of this calibration since the $\Gamma_{\gamma 0}$ are calibrated to the $^2H(\gamma, n)$ cross section. In fact, we observed a $\Gamma_{\gamma 0}$ of 3.5 eV for the 40.7-keV resonance. The present work is in excellent agreement with the previous photoneutron experiments. The total strengths for the resonances observed in Refs. 1 and 5 are the final entries in the table. If we scale these sums for the new value of the 40.7-keV resonance, then the Livermore and Toronto measurements bracket the present strength measurements. (See the values in parentheses in Table III.) The Livermore result would be ~16% lower, and Toronto ~9% higher than the present result. In addition, the angular-distribution ratios for the three independent experiments are in excellent agreement.

The present photoneutron results are not in good agreement with the (n, γ) work.[10,35] The two measurements can be compared in detail since the resolution of the (n, γ) data and the present work are comparable. The (γ, n) and (n, γ) radiative widths are given in Table IV. Clearly, the (n, γ) method consistently overestimates the strengths. The strengths from the (n, γ) method are larger than the present results by a factor of approximately 1.6. This implies that the $M1$ and $E2$ strengths reported in Refs. 10, 35, and 36 for ^{208}Pb are too large by about 1.6.

TABLE II. Results of the present high-resolution photoneutron experiment.

E_n (keV)	E_γ (MeV)	R $\sigma(90°)/\sigma(135°)$	J^π	$g_\gamma \Gamma_{\gamma 0} \Gamma_n/\Gamma$ (eV)	$\Gamma_{\gamma 0}$ (eV)
992	8.367	1.3 ±0.12	1^{-} [a]	5.15	3.7
985	8.360	1.4 ±0.18	$1, 2^{+}$	2.86	1.91, 1.15
971	8.346	1.3 ±0.2	$1, 2^{+}$	1.43	1.0, 0.6
966	8.341	0.67 ± 0.13	$1, 2^{+}$	0.40	0.27, 0.16
947	8.322	1.53 ± 0.13	1^{-} [a]	4.44	3.0
938	8.313	1.06 ± 0.13	$1, 2^{+}$	1.35	0.9, 0.5
921	8.295	1.48 ± 0.24	$1, 2^{+}$	0.41	0.3, 0.2
902	8.276	1.64 ± 0.15	1^{-} [a]	2.88	1.9
891	8.265	0.75 ± 0.13	$1, 2^{+}$	0.41	0.27, 0.16
879	8.253	1.25 ± 0.29	$1, 2^{+}$	0.37	0.25, 0.15
849	8.223	1.20 ± 0.12	$1, 2^{+}$	2.61	1.7, 1.0
840	8.214	1.67 ± 0.16	1^{-} [a]	6.17	4.1
834	8.208	1.03 ± 0.11	$1, 2^{+}$	1.69	1.1, 0.7
830	8.204	0.63 ± 0.09	$1, 2^{+}$	0.55	0.37, 0.22
813	8.187	1.18 ± 0.19	$1, 2^{+}$	0.69	0.46, 0.28
773	8.147	1.17 ± 0.21	2^{+} [c]	0.38	0.25
731	8.105	1.29 ± 0.13	1^{-} [a]	3.04	2.0
721	8.094	1.40 ± 0.18	$1, 2^{+}$	0.85	0.57, 0.34
694	8.067	1.44 ± 0.12	$1, 2^{+}$	3.92	3.1, 1.9
647	8.020	1.20 ± 0.06	1^{-} [a]	10.37	6.9
638	8.011	1.16 ± 0.21	2^{+} [d]	0.20	0.13
630	8.003	1.51 ± 0.18	$1, 2^{+}$	0.40	0.27, 0.16
610	7.983	1.57 ± 0.08	1^{-}	13.39	8.9
600	7.973	1.46 ± 0.09	1^{-} [a]	7.43	5.5
594	7.967	0.72 ± 0.09	$1, 2^{+}$	0.37	0.25, 0.15
548	7.921	0.73 ± 0.04	$1, 2^{+}$	3.69	2.5, 1.5
543	7.916	0.87 ± 0.08	2^{+} [c]	0.94	0.38
537	7.910	1.23 ± 0.06	1^{-} [a]	9.17	6.1
499	7.871	1.14 ± 0.13	$1, 2^{+}$	0.81	0.54, 0.32
488	7.860	1.03 ± 0.09	$1, 2^{+}$	1.91	1.3, 0.8
481	7.853	0.91 ± 0.08	$1, 2^{+}$	1.81	1.2, 0.7
449	7.821	1.2 ±0.2	$1, 2^{+}$	4.0	2.6, 1.6
425	7.797	1.3 ±0.15	$1, 2^{+}$	1.3	0.87, 0.52
419	7.791	1.9 ±0.2	1^{+} [b]	0.8	0.53
332	7.704	1.2 ±0.15	1^{+} [b]	0.75	0.50
313.7	7.685	1.15 ± 0.05	1^{-} [a]	9.6	6.4
295	7.666	0.99 ± 0.1	1^{+} [b]	0.57	0.40
281.0	7.652	1.8 ±0.2	$1, 2^{+}$	0.43	0.29, 0.17
253.6	7.625	0.98 ± 0.10	1^{-} [a]	19.6	13.1
246	7.617	0.67 ± 0.07	$1, 2^{+}$	1.64	1.1, 0.66
179	7.550	1.51 ± 0.15	1^{-} [a]	10.9	7.3
154.8	7.526	1.72 ± 0.17	1^{+} [b]	0.69	0.46
129.6	7.500	1.03 ± 0.10	1^{+} [b]	1.14	0.76
125.8	7.485	1.78 ± 0.18	1^{+} [b]	2.1	1.4
114.1	7.494	1.49 ± 0.15	1^{+} [b]	1.7	1.1
101.3	7.472	1.61 ± 0.16	$1, 2^{+}$	0.23	0.15, 0.09
89.6	7.460	1.97 ± 0.20	1^{+} [b]	2.0	1.3
47.7	7.418	0.53 ± 0.05	2^{+} [c]	0.06	0.02
40.7	7.411	0.92 ± 0.09	1^{-} [b]	5.2	3.5
37.2	7.407	0.67 ± 0.07	1^{+} [b]	0.96	0.64
30.1	7.400	1.5 ±0.15	$1, 2^{+}$	0.3	0.2, 0.12
16.6	7.307	1.3 ±0.13	1^{+} [b]	0.02	0.01

[a] Assignments are based on photoneutron polarization observations, Refs. 6 and 7.
[b] Assignments are taken from Refs. 9, 10, and 35.
[c] Assignments are from Ref. 36.

TABLE III. Comparison of photoneutron experiments with the present work. The values in parentheses have been renormalized to the strength of the 40.7-keV resonance determined from the present work.

E_n (keV)	Argonne R	Argonne $\Gamma_{\gamma 0}$ (eV)		Livermore R	Livermore $\Gamma_{\gamma 0}$ (eV)	Toronto R	Toronto $\Gamma_{\gamma 0}$ (eV)
30.1	1.5 ± 0.15	0.2		1.41 ± 0.2	0.2	1.10 ± 0.17	0.4
37.2	0.67 ± 0.07	0.64		0.64 ± 0.09	0.56 [a]	0.74 ± 0.14	1.0
40.7	0.92 ± 0.09	3.5		1 [b]	4.2 [c] (3.5)	0.88 ± 0.07	4.2 [c] (3.5)
89.6	1.97 ± 0.20	1.3				1.25 ± 0.09	0.9
114.1	1.49 ± 0.15	1.1		1.54 ± 0.22	1.4	1.23 ± 0.14	0.9
179	1.51 ± 0.15	7.3		1.53 ± 0.22	11.0	1.37 ± 0.05	11.8
246	0.67 ± 0.07	0.66	13.8	1.10 ± 0.15	15.3	1 [b]	17.7
253.6	0.98 ± 0.10	13.1					
295	0.99 ± 0.10	0.4				1.09 ± 0.16	1.7
313.7	1.15 ± 0.05	6.4		1.12 ± 0.16	6.7	1.10 ± 0.07	7.0
600	1.46 ± 0.09	5.5	14.4	1.81 ± 0.25	12.8	1.60 ± 0.17	21.2
610	1.57 ± 0.08	8.9					
647	1.20 ± 0.06	6.9		1.26 ± 0.18	5.5	1.24 ± 0.22	6.7
834	1.03 ± 0.11	1.1					
840	1.67 ± 0.16	4.1	6.9	1.49 ± 0.21	6.8	1.53 ± 0.37	7.3
849	1.20 ± 0.12	1.7					
	Total	62.84			64.46(53.7)		80.8(67.3)

[a] This value was obtained by assuming that this resonance is a dipole excitation.
[b] The angular distributions were normalized to unity for these resonances in Refs. 1 and 5.
[c] The values of $\Gamma_{\gamma 0}$ were normalized to the strength of the 40.7-keV resonance in Refs. 1 and 5.

III. PHOTONEUTRON POLARIZATION STUDIES

A. Threshold photoneutron polarization method

The photoneutron polarization method is a powerful tool for determining the parities of photoexcitations near threshold. This method was developed[37] at Argonne for application to the threshold region of the $^{208}Pb(\gamma, \vec{n}_0)^{207}Pb$ reaction. The photoexcitation properties of ^{208}Pb are diagrammed in Fig. 5 for dipole and electric quadrupole resonances in ^{208}Pb. The $E1$ photon excites a 1^- resonance which can decay by s- or d-wave neutrons. Therefore, the angular distribution for the photoneutron reaction in ^{208}Pb for 1^- resonance will, in general, be nonisotropic. In fact, the angular-distribution ratio $[R \equiv \sigma(90^\circ)/\sigma(135^\circ)]$ for $E1$ excitations in ^{208}Pb varies between 0.67 and 2.0. An $M1$ excitation excites 1^+ levels and leads to p_0- and p_1-wave neutron decay, where the subscripts refer to the channel spin of the neutron-nucleus system. Of course, the angular distribution of photoneutrons from these levels is also, generally, nonisotropic and the angular-distribution ratio has an identical range. Thus, a measure of the angular distribution for resonances in ^{208}Pb reveals nothing of the parities of the levels. The $E2$ photon excites 2^+ resonances which can decay by p_1 or f_0 neutrons. If one can ignore the f-wave decay, then the angular-distribution ratio for 2^+ resonances is 0.67. However, a measure of the cross section over the complete angular range would be more suitable for assigning the spins of resonances.

The advantages of observing the photoneutron polarization can be seen by considering the expression[38] for the differential polarization for the $^{208}Pb(\gamma, \vec{n}_0)^{207}Pb$ reaction:

$$d\vec{p}/d\Omega = \hat{k}\,\lambda_\gamma^2\{[-0.325a_s(E1)\,a_{p0}(M1)\sin\Delta_{sp0} + 0.23a_s(E1)\,a_{p1}(M1)\sin\Delta_{sp1} - 0.23a_d(E1)\,a_{p0}(M1)\sin\Delta_{dp0} - 0.325a_d(E1)\,a_{p1}(M1)\sin\Delta_{dp1}]\sin(\theta) - 0.199[a_s(E1)\,a_d(E1)\sin\Delta_{sd} + a_{p0}(M1)\,a_{p1}(M1)\sin\Delta_{p0\,p1}]\sin(2\theta)\}. \quad (1)$$

Here, $\hat{k}$ is a unit vector which is perpendicular to the reaction plane, $a_{ls}(\mathfrak{M}\mathfrak{L})$ are the reaction amplitudes for the emission of a photoneutron of orbital angular momentum l and channel spin s. It is clear from the above expression that an $E1$-$M1$ interference gives rise to an angular dependence of $\sin(\theta)$, whereas an $E1$

excitation leads to a $\sin(2\theta)$ dependence. However, we make the observation that Δ_{p0p1}, the nonresonant phase difference for p waves, is approximately zero: $\Delta_{p0p1}=\phi_{p0}-\phi_{p1}\approx 0$. If the nonresonant phase shifts are approximated by hard-sphere phase shifts then $\Delta_{p0p1}=0$. With this approximation the differential polarization for dipole photoexcitation becomes

$$\frac{d\vec{p}}{d\Omega}\approx\hat{k}\,\lambda\!\!\!^{-}_{\gamma}{}^2\{[-0.325a_s(E1)\,a_{p0}(M1)\sin\Delta_{sp0}+0.23a_s(E1)\,a_{p1}(M1)\sin\Delta_{sp1}-0.23a_d(E1)\,a_{p0}(M1)\sin\Delta_{dp0}$$
$$-0.325a_d(E1)\,a_{p1}(M1)\sin\Delta_{dp1}]\sin(\theta)-0.199a_s(E1)\,a_d(E1)\sin\Delta_{sd}\sin(2\theta)\}. \qquad (2)$$

The angular dependence of the photoneutron polarization provides a signature for the multipolarity of the resonance. A pure $M1$ excitation gives no polarization, a pure $E1$ resonance gives rise to a $\sin(2\theta)$ angular dependence, and interfering $E1$ and $M1$ excitations lead to a $\sin(\theta)$ dependence. In a region where only dipole radiation is a consideration, a measurement of the photoneutron polarization at only two angles, $\theta=90°$ and $135°$, is necessary in order to determine the multipolarity of the photoexcitation process. An $E1$-$E2$ interference effect can give rise to $\sin(\theta)$ and $\sin(3\theta)$ terms in the differential polarization and, in general, cannot be distinguished from $E1$-$M1$ interference by observing the polarization at only two angles.

TABLE IV. Comparison of present ground-state radiation widths with those of the fast-neutron capture method.

E_n (keV)	E_γ (MeV)	J^π	Argonne $\Gamma_{\gamma 0}$ (eV)	Oak Ridge $\Gamma_{\gamma 0}$ (eV)
16.6	7.397	1^+	0.01	0.07
30.1	7.410	$1, 2^+$	0.2	0.64
37.2	7.417	1^+	0.64	0.76
40.7	7.421	1^-	3.5	5.07
47.7	7.418	2^+	0.02	0.035
89.6	7.470	1^+	1.3	2.01
101.3	7.481	$1, 2^+$	0.15	0.32
114.1	7.494	1^+	1.1	1.55
125.8	7.496	1^+	1.4	2.59
129.6	7.510	1^+	0.76	0.95
154.8	7.535	1^+	0.46	0.66
179	7.559	1^-	7.3	15.8
253.6	7.625	1^-	13.1	21.1
295	7.666	1^+	0.40	0.71
313.7	7.685	1^-	6.4	10.1
332	7.704	1^+	0.50	1.19
419	7.791	1^+	0.53	0.58
488	7.860	$1, 2^+$	1.3	1.6
537	7.910	1^-	6.1	7.2
543	7.916	2^+	0.38	0.2
600	7.973	1^-	5.5	9.9
610	7.983	1^-	8.9	14.0
638	8.011	2^+	0.13	0.56
647	8.020	1^-	6.9	9.3
694	8.067	$1, 2^+$	3.1	3.2
721	8.094	$1, 2^+$	0.57	1.1
731	8.105	1^-	2.0	3.1
773	8.147	2^+	0.25	0.51
840	8.214	1^-	4.1	7.0
902	8.276	1^-	1.9	4.4
947	8.322	1^-	3.0	5.4
992	8.367	1^-	3.7	5.6
		$\sum\Gamma_{\gamma 0}$	85.6	137.2

Most of the $M1$ transition strength reported in the early Livermore photoneutron data[1] occurred in five resonances between 180 and 1000 keV. Experimental forays into this alleged giant $M1$ resonance region have been redoubled in recent years. In particular, the photoneutron polarization experiments[6,7] were the first results which demonstrated the absence of large amounts of $M1$ strength in this excitation region of ^{208}Pb. For this reason, we wish to briefly review the findings of the threshold photoneutron polarization method.

Unfortunately, no single neutron polarimeter can span the entire energy range of interest. Consequently, a variety of analyzing targets was used for these experiments. Photoneutrons were scattered from natural Mg in the energy range 170–320 keV and from ^{16}O between 500 and 1200 keV. Above 1.5 MeV a carbon scatterer was employed. A schematic diagram of the Argonne threshold photoneutron facility and polarimeter system is shown in Fig. 6. In these experiments the linac was operated in a mode which produced electron bursts

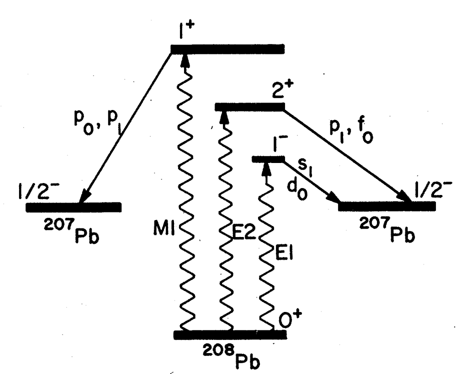

FIG. 5. Photoexcitation processes of ^{208}Pb. The labels ls refer to the orbital angular momenta and channel spin of the neutron decay.

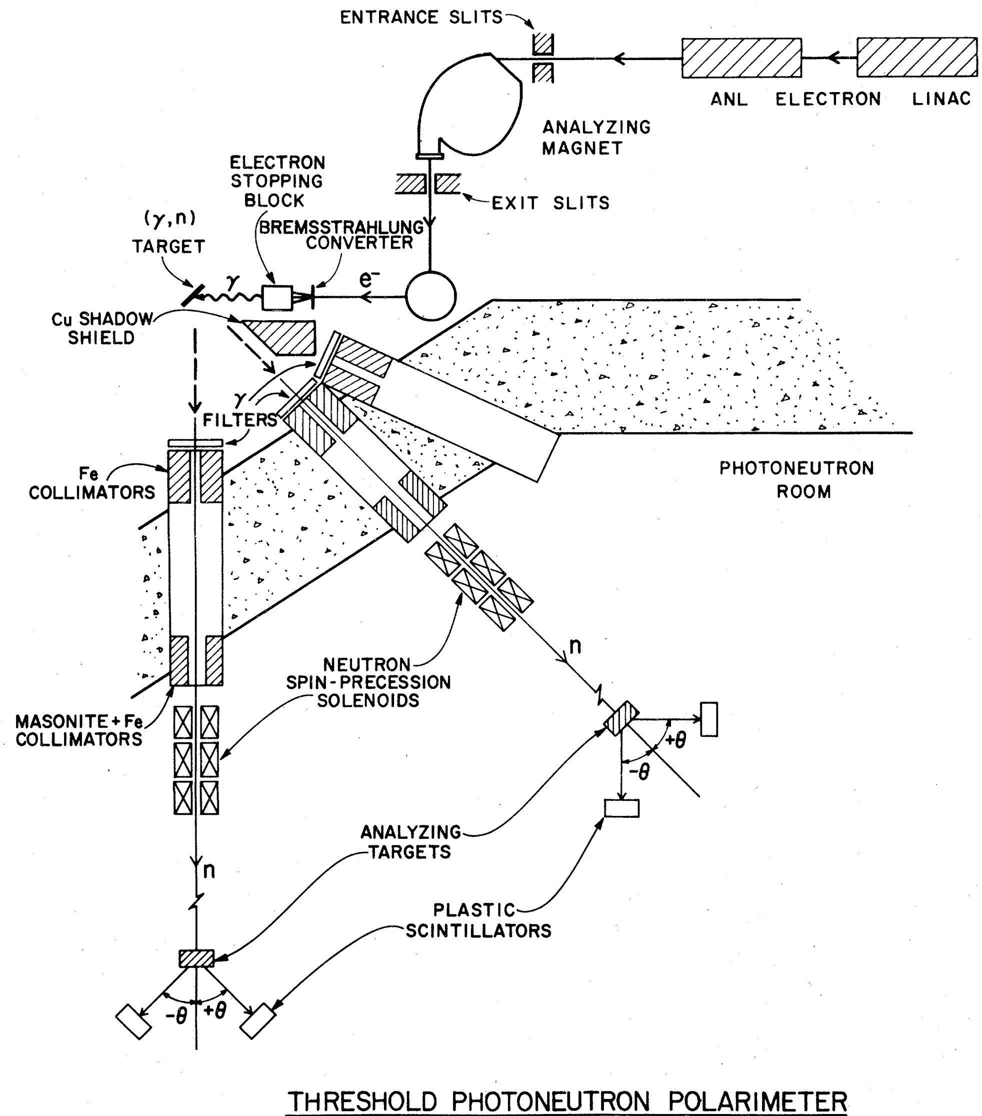

FIG. 6. Schematic diagram of the threshold photoneutron facility and polarimeter system at the Argonne National Laboratory.

of 4-ns duration and 10-A peak current at a rate of 800 Hz. The energy-analyzed electron beam was focused onto an Ag converter, and the bremsstrahlung from this process irradiated the enriched (99.1%) metallic ^{208}Pb target.

The partially polarized photoneutrons from the $^{208}\mathrm{Pb}(\gamma, \vec{n}_0)^{207}\mathrm{Pb}$ reaction traveled through two well-collimated flight paths which were approximately 9 m in length and were at reaction angles of 90° and 135° with respect to the photon beam axis. The neutrons also passed through a neutron spin-precession solenoid.[37] Finally, the neutrons scatter from the analyzing targets located at the end of each flight path. The neutrons are then detected in plastic scintillators placed at scattering angles of $\pm\theta$, where $\theta = 45°$ for Mg and 50° for ^{16}O and C analyzing targets. Rather than measure the asymmetry in the scattered neutron beam by interchanging the location of the detectors, the detectors were held fixed and the neutron spins were precessed through known angles. The spin precession angle was determined by observing with the time-of-flight spectrometer the amount of time each neutron spent in the solenoid. Thus, this method is compatible for a continuous energy spectrum of neutrons.

B. Polarization results: 180-1000 keV

The results of the threshold photoneutron polarization experiments are summarized in Figs. 7 and

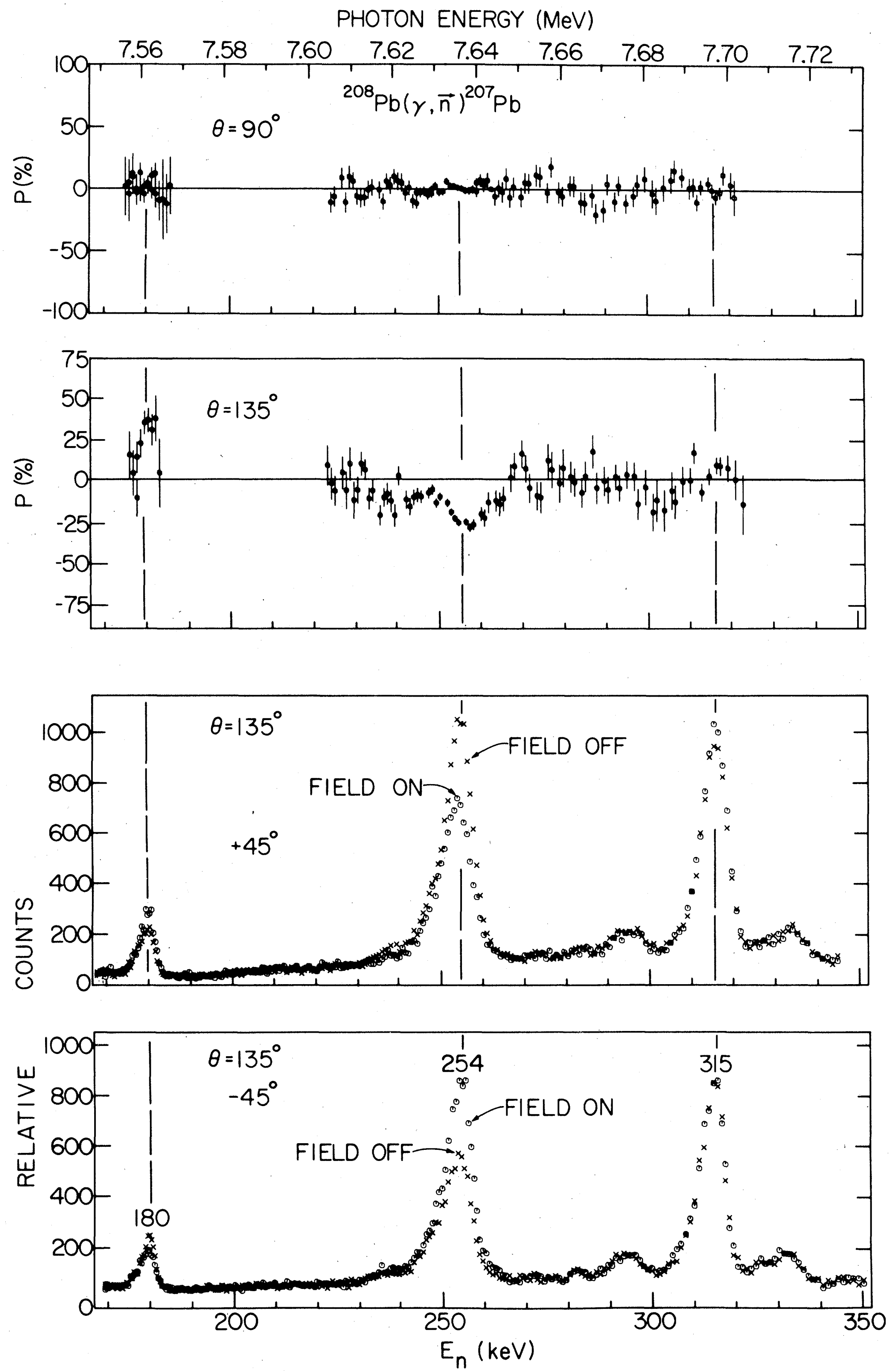

FIG. 7. The two lower panels illustrate the raw time-of-flight data for the $^{208}Pb(\gamma,\vec{n})^{207}Pb$ reaction at an angle of 135° and after the photoneutrons are scattered from a Mg analyzer at angles of ±45°. Both cases of the spin-precession solenoidal field are shown. The final measured photoneutron polarizations are shown in the upper panels.

8. The photoneutron energy region 170–320 keV is shown in Fig. 7. Previous photoneutron experiments indicated that the 179- and 314-keV resonances were $M1$ excitations. The reduced transition probabilities for these resonances would be 1.46 and 1.22 μ_0^2, respectively, if they are $M1$ excitations. These two levels would then account for 17% of the $M1$ sum rule, and consequently, would

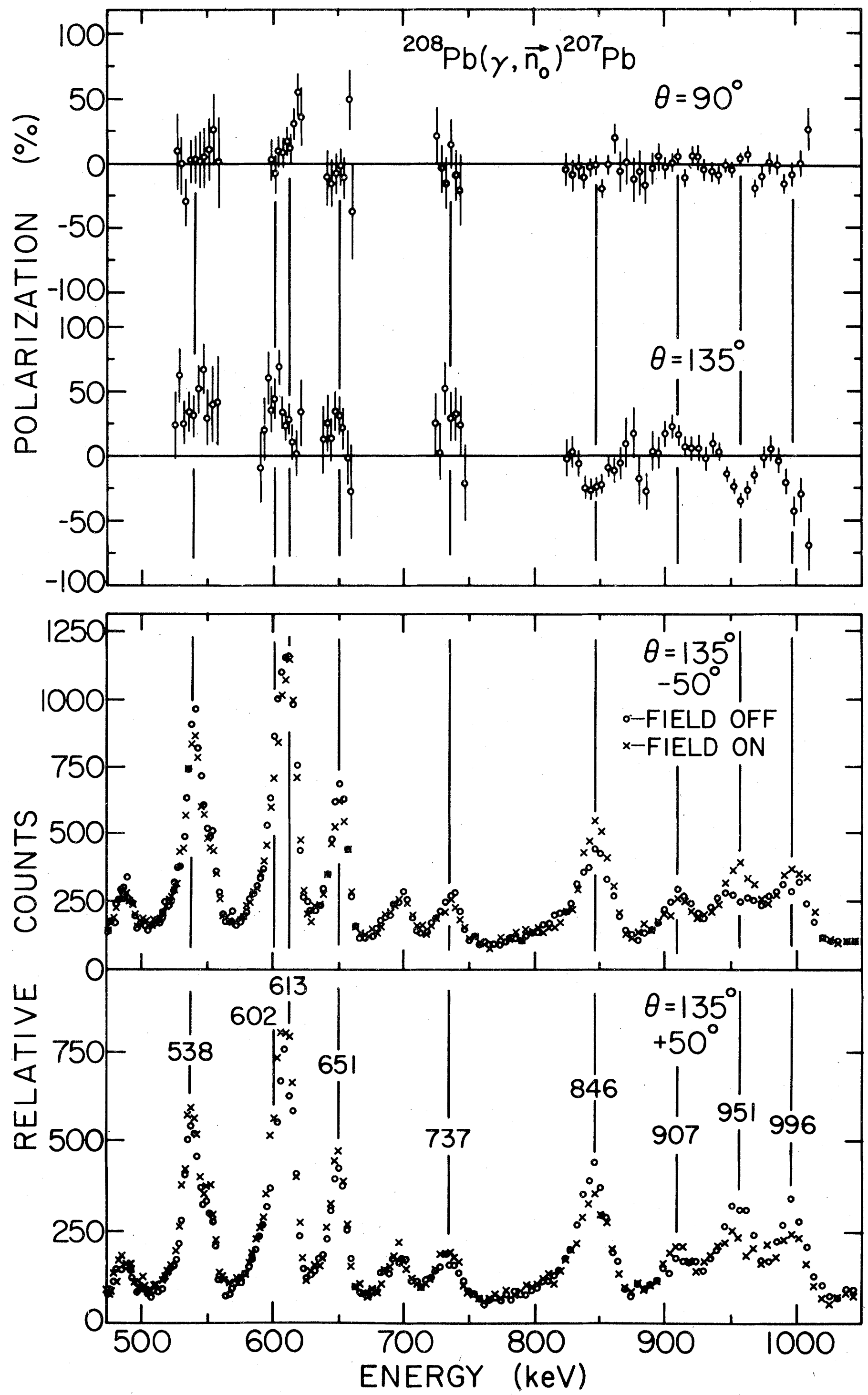

FIG. 8. The photoneutron polarization results obtained by using an ^{16}O analyzer. (See caption of Fig. 7.)

represent a significant amount of $M1$ strength. However, we found that the photoneutron polarization data, given in the two upper panels of Fig. 7, indicate that the 180-, 254- and 314-keV resonances have a vanishing polarization at 90° and a nonzero effect at 135°. The polarization of the neutrons emitted from these resonances have a $\sin(2\theta)$ angular dependence. Therefore, we have assigned these resonances as $E1$ excitations. The lower panels of Fig. 7 demonstrate the clarity with which the photoneutron polarization near threshold can be measured with the Argonne high-current linac. These panels show the photoneutron spectra for the $^{208}Pb(\gamma, \vec{n})^{207}Pb$ reaction at an angle of 135° after the photoneutrons have scattered from a natural Mg target at angles of ±45°.

The data in the lower panels show the effect with the solenoidal field off and on. In this case, the solenoid field was set to precess the spin of a 250-keV neutron through 180°. The effect is most dramatic for the 254-keV resonance. The 254-keV resonance is a well-known $E1$ excitation. The large polarization effect is due to a large s-d-wave admixture in the outgoing neutron channel. The 180-keV resonance also exhibits a large polarization and, consequently, a large s-d-wave admixture. This effect was discovered[39] in the photoneutron polarization data and confirmed in neutron scattering measurements. These findings will be discussed in detail in Sec. V A.

There are no photoneutron polarization data for the energy region 320–500 keV. This is due to the fact that the resonances in this energy region have small ground-state radiative widths which renders the photoneutron polarization method unfeasible. The photoneutron polarization observations between 500 and 1000 keV are displayed in Fig. 8.

Before the photoneutron polarization was observed in this energy region, the 538-, 600-, 610-, 647-, and 840-keV resonances were suspected[1,5] of comprising a large fraction of the giant $M1$ resonance. Again, the observed polarizations are shown in the upper panels of Fig. 8 for angles of 90° and 135°. All of the major resonances in this energy region exhibit a nonzero polarization at 135°, whereas all these resonances with the exception of the 610-keV resonance give rise to no polarization at 90°. Consequently, the resonances at 537, 600, 647, 731, 840, 902, 947, and 992 were assigned as $E1$ excitations, contrary to the Livermore and Toronto findings. However, as already emphasized in Sec. III A, the photoneutron angular-distribution measurements provide no determination of the parities of dipole resonances in this energy region of ^{208}Pb. The polarization data could not rule out an $M1$ assignment for the 610-keV resonance, since there is clearly a nonzero polarization at the reaction angle of 90°. This was interpreted[6] as $E1$-$M1$ interference where the 610-keV level is an $M1$. The high-resolution photoneutron work clearly indicates that the 610-keV resonance is $E1$ in nature as discussed in Sec. II B.

C. Photoneutron polarization above 1 MeV

The photoneutron polarization for the $^{208}Pb(\gamma, \vec{n}_0)/^{207}Pb$ reaction was observed[8] in the energy range 1 to 2 MeV above threshold and at an angle of 90°. Above an excitation energy of 8.4 MeV in ^{208}Pb individual levels can no longer be resolved. In this energy range, we looked only for $E1$-$M1$ interference patterns, i.e., a nonzero polarization effect at a reaction angle of 90°. The results of this experiment are summarized in Fig. 9. The raw time-of-flight spectra after the photoneutrons scattered from either ^{16}O or natural C are shown in the top panel of that figure. Three different electron end-point energies—9.0, 9.6, and 10.2 MeV—were selected in order to eliminate the effects of non-ground-state photoneutron transitions. The lower panel illustrates the analyzing powers of the scatterers used in the measurement. The final deduced polarizations are shown in the central panel. Indeed, there are many regions in this energy range which exhibit a significant polarization effect. This is a definite indication of non-$E1$ strength. Of course, since the level structure is not fully resolved and since the photoneutron polarization was observed at only one angle, one cannot distinguish whether the polarization is due to $E1$-$M1$ or $E1$-$E2$ interference. Most importantly, these data illustrate the potentially most fruitful locations for future searches for $M1$ excitations in ^{208}Pb. Over the past eight years the predicted location of the giant $M1$ resonance in ^{208}Pb has migrated from 7.5 to 10 MeV. Thus, methods must be developed for determining the amount of $M1$ strength in the excitation energy range above 9 MeV, if we are to fully understand the nature of the collective $M1$ excitation in ^{208}Pb.

IV. COLLECTIVE MAGNETIC DIPOLE EXCITATIONS IN ^{208}Pb

A. Theoretical developments

Most simply the giant $M1$ resonance in ^{208}Pb can be described as a combination of both proton and neutron spin-flip excitations. The wave function for the isovector component can be written as

$$|1^+\rangle_v = a|h_{11/2}{}^{-1}h_{9/2}\rangle_\pi - b|i_{13/2}{}^{-1}i_{11/2}\rangle_\nu$$

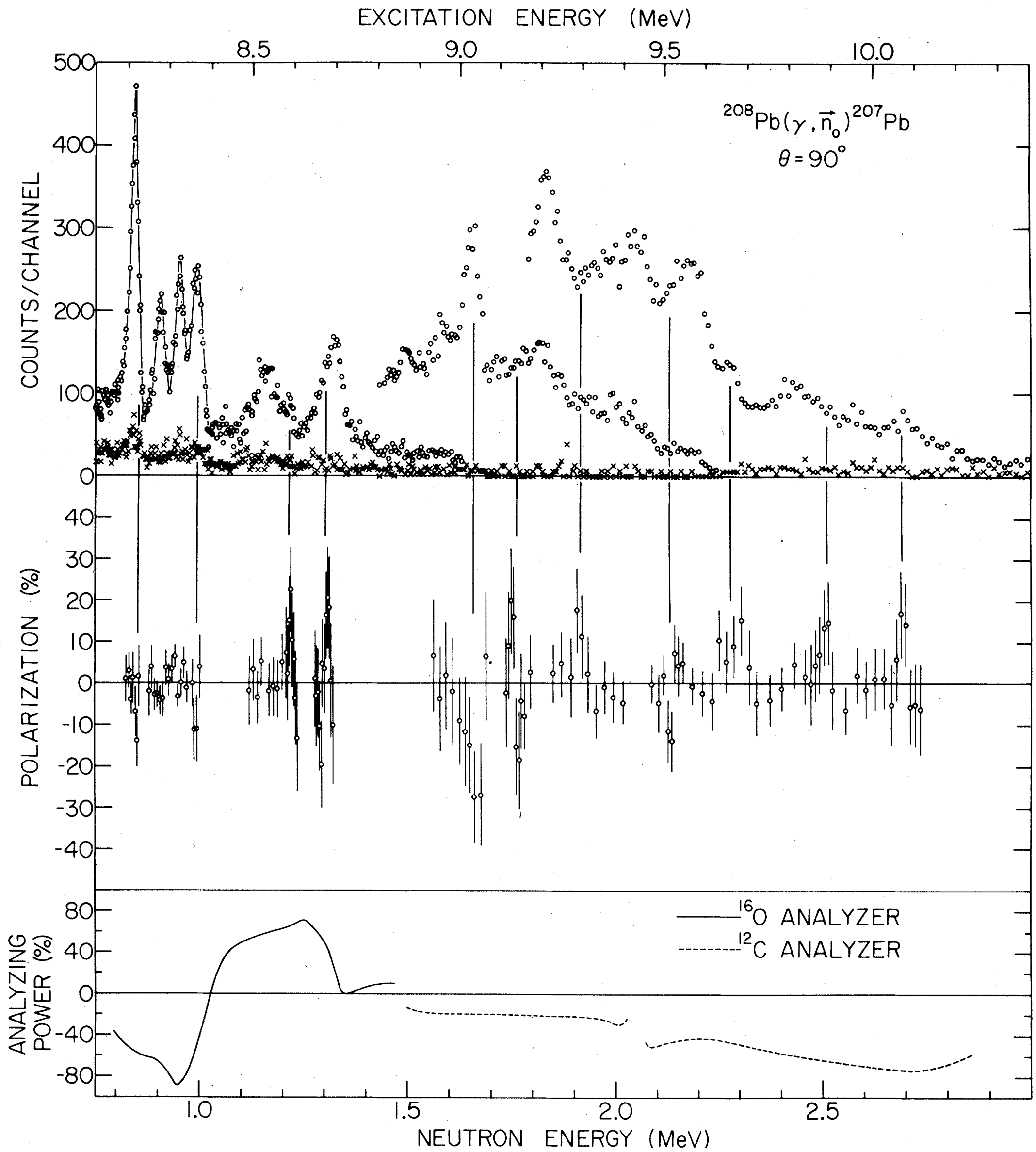

FIG. 9. Photoneutron polarization results above 8.4 MeV in ^{208}Pb. The lower panel illustrates the analyzing powers of the targets employed in this energy range. The central panel illustrates the final polarization results at $\theta = 90°$. The upper panel is the raw time-of-flight data. The symbol x represents the observed background.

and isoscalar

$$|1^+\rangle_s = a|h_{11/2}{}^{-1}h_{9/2}\rangle_\pi + b|i_{13/2}{}^{-1}i_{11/2}\rangle_\nu .$$

The $M1$ reduced transition probability can be determined from the definition

$$B(M1; 1^+ \to 0^+) \equiv \tfrac{1}{3}|\langle 0^+\|M1\|1^+\rangle|^2 ,$$

where

$$\langle 0^+\|M1\|1^+\rangle_{s,v} = -\left(\frac{3}{4\pi}\right)^{1/2}\left(\frac{e\hbar}{2M_pc}\right)[(g_{s_p}-g_{l_p})(2j_p+1)^{1/2}\langle j_p, \tfrac{1}{2}|M1|j_p+1, \tfrac{1}{2}\rangle\, a$$
$$\pm (g_{s_n}-g_{l_n})(2j_n+1)^{1/2}\langle j_n, \tfrac{1}{2}|M1|j_n+1, \tfrac{1}{2}\rangle\, b] .$$

Here, the g_s and g_l are the spin and orbital g factors, respectively. Then the reduced transition probability becomes

$$B(M1;1^+\to0^+)_{s,v}=\frac{\mu_0^2}{2\pi}\left\{(g_{s_p}-g_{l_p})\left[\frac{l_p(l_p+1)}{2l_p+1}\right]^{1/2}a\pm(g_{s_n}-g_{l_n})\left[\frac{l_n(l_n+1)}{2l_n+1}\right]^{1/2}b\right\}^2, \tag{3}$$

where the components of the wave function a and b can be determined from shell-model calculations, e.g., Ref. 22. The $M1$ sum rule can be calculated from the above expression using the bare $M1$ operator, i.e.,

$$g_{s_n}=-3.82,\quad g_{s_p}=5.58,$$
$$g_{l_n}=0,\quad g_{l_p}=1.$$

The sum rule is then given by

$$B_{\rm SR}(M1;1^+\to0^+)=16.6\,\mu_0^2.$$

Many of the theories of the collective $M1$ excitation have this simple argument of configuration mixing embedded in them.

Having followed the configuration-mixing approach of Arima and Horie,[40] Vergados[22] calculated the $M1$ strength in ^{208}Pb using the Hamada-Johnston interaction. Although a larger set of p-h basis states were used in the calculation than in the simple example above, the contribution to the $M1$ transition probability was dominated by the $|0h_{11/2}{}^{-1}0h_{9/2}\rangle$ and $|0i_{13/2}{}^{-1}0i_{11/2}\rangle$ configurations. Moreover, Vergados predicted that the isovector component, located at 7.52 MeV, should have $B(M1;1^+\to0^+)=16.02\,\mu_0^2$, which nearly exhausts the $M1$ sum rule. The isoscalar component was predicted to have only $0.4\,\mu_0^2$ at an energy of 5.45 MeV. This calculation was in apparent qualitative agreement with the early photoneutron experiments at Livermore.

The experimental results available at that time indicated that the $M1$ resonance occurred in several large levels and this fragmentation was difficult to understand. Lee and Pittel[23] demonstrated that the inclusion of 2p-2h configurations can cause significant fragmentation of the 1p-1h giant $M1$ resonance. In that theory, the 1p-1h portion of the calculation was identical to that of Vergados so that the transition probability and centroid of the resonance are the same as those of Ref. 22. However, this theory could not explain the large amount of spreading that was believed[1] to pervade the alleged $M1$ giant resonance in ^{208}Pb.

In a different approach Ring and Speth[24] employed effective $M1$ operators and a density-dependent Migdal interaction in order to describe the magnetic properties of nuclei in the mass-208 region. Although the effect was small, meson-exchange corrections were also included in that calculation. This method allowed them to accurately predict the values of magnetic moments in these heavy nuclei. In addition, they predicted results for the GMDR in ^{208}Pb. The transition probability was found to be only about one-third of that predicted by Vergados. Moreover, the energies of the excitations were expected to be significantly higher than those of Vergados' calculation. These higher energy excitations are chiefly due to the effective p-h interaction used by Ring and Speth. The form of this interaction is

$$\frac{2k_F m^*}{\pi^2}F_{\rm ph}=(f_0+f_0'\vec\tau_1\cdot\vec\tau_2+g_0\vec\sigma_1\cdot\vec\sigma_2+g_0'\vec\sigma_1\cdot\vec\sigma_2\vec\tau_1\cdot\vec\tau_2)\,\delta(r), \tag{4}$$

where f_0 and f_0' were allowed to be density dependent and the g_0 and g_0' were determined by fitting the values of the magnetic moments in the Pb region. With this interaction, the isovector and isoscalar components of the GMDR were expected to occur at 8.31 MeV with $B^{\downarrow}(M1)=3.67\,\mu_0^2$, and 7.50 MeV with $1.89\,\mu_0^2$, respectively. Clearly, the predicted magnetic excitations of ^{208}Pb depend critically upon the theoretical approach.

Knüpfer *et al.* also speculated that the $M1$ strength in ^{208}Pb might be quenched. In particular, they observed that the amount of $M2$ strength in nuclei depends on the mass and is strongly quenched in ^{208}Pb. The quenching effect was parametrized by small values of the effective spin g factors. If these effective g factors are decreased, then the amount of $M1$ strength is also reduced. The effective g factors which are suggested by Ref. 12 are given by

$$g_{sn}^{\rm eff}=-2.29,\quad g_{sp}^{\rm eff}=3.35,$$
$$g_{ln}^{\rm eff}=-0.031,\quad g_{lp}^{\rm eff}=1.119.$$

If these values are used in Eq. (3) instead of the free-nucleon g factors, then the effective sum rule for these effective values becomes

$$B_{\rm SR}^{\downarrow\,\rm eff}=4.8\,\mu_0^2$$

This value is approximately 30% of the $M1$ sum rule in ^{208}Pb. This is close to the value of $5.56\,\mu_0^2$ which was predicted by Ring and Speth. There have been no conjectures that the $M1$ resonance is quenched to a lower value than approximately

30% of the sum rule. Nevertheless, below 8.4 MeV only about 14% of the $M1$ sum rule can be accounted for experimentally.

From a different viewpoint, Bohr and Mottelson[25] argued that collective vibrational excitations in the nucleus are governed by a sustained motion in the nucleonic density excited by variations in the one-body operator and vice versa. The one-body operator in the case of $M1$ excitations is, of course, the spin-dependent part of the p-h interaction. The change that this spin-field has upon the one-body potential perturbs the restoring force for the vibrational mode. This leads to a perturbed energy $\hbar\omega$ for the isovector oscillation of the form

$$E_R = V_{so}\left(1+\frac{k\Sigma}{V_{so}}\right)^{1/2},$$

where V_{so} is the unperturbed energy or the spin-orbit splitting, $k=40/A$, and

$$\sum = \frac{16}{3}\left[\frac{l_n(l_n+1)}{2l_n+1}+\frac{l_p(l_p+1)}{2l_p+1}\right] \approx \tfrac{8}{3}(2\bar{l}+1).$$

Here $\bar{l}\equiv(l_p+l_n)/2$ is the average orbital angular momenta of the nucleons. This formulation provides a convenient method for predicting the location of the isovector part of the GMDR as a function of mass number. For ^{208}Pb, the GMDR would be expected at $E_{exc}=8.1$ MeV. In addition, the $M1$ transition probability would be expected to be quenched by a factor of V_{so}/E_R, so that $B^{\uparrow}(M1)\simeq 12\,\mu_0^2$. The theoretical predictions are summarized in Table V.

Dehesa, Speth, and Faessler[26] improved upon the analysis of Ring and Speth by coupling of the 1p-1h excitations to the 2p-2h states. They obtained a dramatic splitting of the magnetic dipole states in ^{208}Pb. In particular, they predicted that approximately 30% of the $M1$ strength is distributed over many levels above 8 MeV. We note that this prediction is consistent with the observation of significant photoneutron polarizations above 8 MeV. Of course, these data alone do not provide an adequate test of the theory. Even though the GMDR was split into numerous fragments, the theory predicted that there should be at least two large concentrations of $M1$ strength. The theory showed that the distribution of $M1$ strength in these large levels depends sensitively upon the spin-dependent pieces of the p-h interaction, especially the very weak spin-dependent proton-neutron interaction. Thus far, no large $M1$ excitations in ^{208}Pb have been observed.

Anastasio and Brown[27] pointed out that the reason that the Ring-Speth approach predicts higher energies than that of Vergados is due to the fact that the spin-dependent parameters in the Migdal interaction, Eq. (4), are larger than one can derive from a phenomenological potential, e.g., Reid soft core or Hamada-Johnston interaction. Furthermore, they demonstrated that the largest contributions to the spin-dependent parameters are from ρ-meson exchange effects. In particular, it was found that the tensor ρ-nucleon coupling gives rise to the largest perturbation of the $M1$ resonance energy through the $\vec{\sigma}_1\cdot\vec{\sigma}_2\,\vec{\tau}_1\cdot\vec{\tau}_2$ term in Eq. (4). This theory predicted the isoscalar and isovector segments of the GMDR to be at 8.37 and 9.21 MeV, respectively. This places the resonances in an energy range where data are sparse and the measurements are extremely difficult. Our knowledge of non-$E1$ excitations in this energy region comes only from photoneutron polarization data[8] and inelastic electron scattering observations.

In the most recent theoretical development Brown and Speth[28] argued that the unperturbed energies that are used in the p-h model may not correspond to empirically determined single-particle energy differences. In that theory the effective mass m^* can deviate significantly from the nucleon mass m if the excitations are above the Fermi surface. For example, $m^*/m \gtrsim 1.0$ for single-particle excitations near the Fermi level and m^*/m decreases to ~0.6–0.7 for excitations approximately $E=\hbar\omega$ above the Fermi level. In fact, an approximation for the effective mass was given:

$$m^*/m=(m^*/m)_B+(\delta m^*/m)/(1+E/2\hbar\omega)^2,$$

where $(m^*/m)_B$ refers to the Brueckner-Bethe effective mass of 0.6–0.7 and $(\delta m^*/m)$ is the con-

TABLE V. Summary of theoretical predictions of magnetic dipole excitation in ^{208}Pb.

Authors	Isoscalar E_{exc} (MeV)	Isoscalar $B^{\uparrow}(M1)$ (μ_0^2)	Isovector E_{exc} (MeV)	Isovector $B^{\uparrow}(M1)$ (μ_0^2)
Vergados (1970)	5.45	0.40	7.52	16.02
Ring, Speth (1972)	7.50	1.89	8.31	3.67
Bohr, Mottelson (1976)			8.1	12
Anastasio, Brown (1977)	8.37	2.0	9.21	14.6
Brown, Speth (1978)	~6.9		~10.30	

tribution from the coupling of the particles and holes to nuclear vibrations. The coupling to vibrations becomes strongest below or near the Fermi level. This approach accurately predicts the location of the GDR in ^{208}Pb. This theory would place the isoscalar and isovector components at ~6.9 MeV and as high as ~10.3 MeV, respectively. The energy of the isovector component is pushed above the energy range of experimental searches for the GMDR in ^{208}Pb. Studies of $M1$ excitations in this energy range in ^{208}Pb present a serious challenge to the experimentalist. It is clear from an examination of Table V that the nature of the $M1$ excitation in ^{208}Pb can only be determined experimentally. That is, the ability of theories to predict magnetic moments in the Pb region provides little help in understanding the complexity of the $M1$ excitation in ^{208}Pb.

B. Experimental findings

Photoneutron experiments have played an important part in the search for the GMDR in ^{208}Pb. Bowman *et al.*[1] focused attention on ^{208}Pb by claiming that approximately 50% of the $M1$ sum rule was found in resonances within 1 MeV of the (γ, n) threshold. These findings were essentially confirmed up to 620 keV by the photoneutron work of Mizumoto *et al.*[2] The parity assignments of Ref. 1 relied solely upon the observation of the photoneutron angular-distribution ratio $R = \sigma(90°)/\sigma(135°)$ for the observed resonances. It was argued that $E1$ excitations will emit s-wave neutrons and $M1$ excitations, p-wave neutrons. This argument ignores the effects of the d-wave neutron decay component for $E1$ resonances in ^{208}Pb. It became apparent with the work of Toohey and Jackson[3] that a small d-wave component would cause the angular-distribution ratio to differ significantly from unity. This led Toohey and Jackson to conclude that assignments made by this method would be unreliable above 200 keV.

Harvey[4] claimed that the tentative $M1$ assignments at 180 and 314 keV may be in serious question. He found that resonances in measurements of the ^{207}Pb$(n, n)^{207}$Pb total cross section which seemed to match those in the (γ, n) channel have an asymmetric shape, characteristic of s-wave neutron induced resonances. Unfortunately, the photoneutron data available then were not of sufficient energy resolution to permit unambiguous parity assignments with this method. The density of levels observed in the neutron channel far exceeds that of the (γ, n) channel. In addition, a large d-wave component in the neutron scattering channel would also foil this technique. Nevertheless, we now know from the photoneutron polarization results and the high-resolution (γ, n) data reported in this paper that Toohey and Jackson's and Harvey's suspicions were justified. Despite the questions raised in Refs. 3 and 4, Haacke and McNeil[5] observed angular distributions of photoneutrons from ^{208}Pb and concluded that, indeed, there are large $M1$ excitations with $M1$ strength totaling approximately 67.5 eV, more than half the sum rule, below 850 keV. Most importantly, these early photoneutron results indicate a significant nonisotropic angular distribution. This will be shown in Sec. V to be due to large s-d-wave admixtures in the outgoing neutron channel.

The threshold photoneutron polarization experiments demonstrated that the amount of $M1$ strength within 1 MeV of threshold could not be nearly so large as previously believed. As pointed out in Sec. III B, all of the large alleged $M1$ excitations, with the exception of the 610 keV resonance, between 180 and 1000 keV, were shown to be $E1$ resonances. At that time, it appeared that a 1^+ assignment of the 610-keV (E_{exc} = 7.99-MeV) resonance would explain both the (γ, n) angular distributions and polarizations. In a later development, Horen *et al.*[11] demonstrated that the 610-keV assignment may not be valid if there are small "hidden" non-$E1$ resonances which are masked by the dominant levels. Moreover, the 610-keV resonance was given a 1^- assignment in Ref. 11 on the basis of the angular distribution for the ^{207}Pb$(n, n)^{207}$Pb reaction and by coordinating the energy scale with that of (γ, n) or (n, γ) work. As already discussed, this method raised some doubt since the level density excited in the elastic neutron scattering channel is high and since the energy scales must be coordinated to better than 0.5 keV. Furthermore, there could be substantial shifts in the peak cross section for 1^- resonances due to interference with the large nonresonant s-wave background in neutron scattering. However, the present high-resolution results verify with a more direct method that the 610-keV resonance is a 1^- excitation. Knüpfer *et al.*[12] also pointed out that a 1^+ assignment for the 7.99-MeV resonance is inconsistent with high-resolution inelastic electron scattering results. However, this resonance was believed at that time to have approximately twice the strength of the present value. Thus, it was possible that a 1^+ resonance might be confused with a nearby $M2$ excitation. It was also suggested in Ref. 12 that one may not see a large amount of $M1$ strength in ^{208}Pb due to a strong quenching mechanism, which is also responsible for diminishing the $M2$ strength.

The only uncontested $M1$ strength within 1 MeV of threshold occurs in small levels below 400 keV. Horen *et al.*[9] discovered a cluster of $M1$ resonances near 7.5 MeV. They found that $\sum \Gamma_{\gamma 0} = 7.2$ eV in this cluster and associated this with the isoscalar component of the GMDR as predicted by Ring and Speth.[24] The present work indicates that the $M1$ strengths found in Refs. 9 and 10 are overestimated by a factor of approximately 1.6. These $M1$ excitations along with a comparison of the present work are given in Table VI. Raman *et al.* discovered additional small $M1$ excitations up to 400 keV. These are also listed in Table VI. The parity assignments in Refs. 9 and 10 were made on the basis of high-resolution observations of neutron elastic scattering from ^{207}Pb. The spin assignments were taken from neutron total cross section data and (n,γ) studies.

Above 8.4 MeV, our only information concerning the fine structure of non-$E1$ excitations is derived from photoneutron polarization studies,[8] as described in Sec. III C. Specifically, a nonzero polarization at 90° indicates the presence of either an $E2$ or $M1$ resonance. Regions of significant nonzero polarization, marked by the arrows in Fig. 10, were found between 8.4 and 9.4 MeV. In this figure, the high-resolution (γ,n) data are shown in the lower curve and the resolution of the photoneutron polarization data is indicated by the upper spectrum. It was originally speculated that this nonzero polarization must be due to $E1$-$M1$ interference, since it was thought that the interference of relatively large resonances was necessary to produce the large polarization effect. Even the smallest resolved resonances in this energy region are too large to be associated with expected $E2$ excitations[41] in this energy region. Thus, it was concluded that the polarization effect was most probably due to the presence of $M1$ strength. However, Horen *et al.*[11] have shown that a polarization effect can be produced by a large $E1$ level interfering with a small non-$E1$ resonance. In light of these new findings, we can only conclude that the polarization data single out regions which might be the most fruitful in future searches for $M1$ excitations above 8.4 MeV.

TABLE VI. Summary of known $M1$ excitations in ^{208}Pb.

E_n (keV)	E_γ (MeV)	$\Gamma_{\gamma 0}$ [a] (eV)	$B^{\uparrow}(M1)$ $\left(\frac{e\hbar}{2M_p c}\right)^2$
	7.279	0.78	0.18
16.6	7.387	0.01	0.002
37.2	7.407	0.64	0.14
72.3	7.443	(0.02)	(0.004)
89.6	7.460	1.3	0.27
114.1	7.485	1.1	0.23
125.8	7.496	1.4	0.29
129.6	7.500	0.76	0.16
131.0	7.502	(0.04)	(0.008)
144.0	7.515	(<0.02)	(<0.004)
146.8	7.518	(<0.02)	(<0.004)
154.8	7.526	0.46	0.093
166.8	7.538	(0.12)	(0.024)
177	7.548	(0.88)	(0.18)
178	7.550	(1.24)	(0.25)
208.5	7.580	(0.07)	(0.014)
216.2	7.587	(0.08)	(0.016)
227.6	7.599	(<0.02)	(<0.004)
247.5	7.619	(0.18)	(0.035)
281.9	7.653	(0.15)	(0.029)
284.7	7.656	(<0.02)	(<0.004)
295.0	7.666	0.40	0.077
332	7.704	0.50	0.094
367	7.738	(<0.05)	(<0.009)
376	7.747	(<0.05)	(<0.009)
382	7.754	(<0.05)	(<0.009)
419	7.791	0.53	0.097
423	7.795	(<0.07)	(0.013)
	Total	10.96	2.25

[a] The values in parentheses are from Ref. 35 and were not confirmed by the present work. All other values are from the present work.

In the meantime, there were numerous experiments which were designed to study the isoscalar component of the $M1$ resonance below threshold. Swann[13] observed the linear polarization of photons resonantly scattered from the 4.843-MeV resonance in ^{208}Pb. The observed linear polarization was consistent with a 1^+ assignment for the excitation. In a later development, Delvecchio and colleagues[14,15] at Princeton showed that the 4.84-MeV resonance was strongly excited in the (α,α') reaction. They concluded that only a natural parity state could be excited so strongly and, consequently, the state is a 1^- excitation. This is in apparent contradiction with the linear polarization results. In a later article, Swann[16] performed a more refined measurement of the linear polarization. The major improvement was the use of an enriched ^{208}Pb sample. He found that the polarization was inconsistent with either an $E1$ or an $M1$ excitation. Rather, the data suggested that there are two resonances at 4.84 MeV, one $E1$ and one $M1$ resonance. This would explain the inconsistency between the (α,α') and the $(\gamma,\vec{\gamma})$ results. There have been no direct observations of two resonances at this energy. However, the high-resolution inelastic proton scattering results[17] show that if two resonances exist, they must be less than 3 keV apart. It remains uncertain how much, if any, $M1$ strength occurs at 4.84 MeV. Cecil *et al.*[18] demonstrated that there are no unnatural parity states between 5 and 6 MeV. The method of Ref. 18 employed both inelastic α-particle and proton scattering.

Freedman *et al.*[19] observed inelastic proton and deuteron scattering from ^{208}Pb. In that experiment

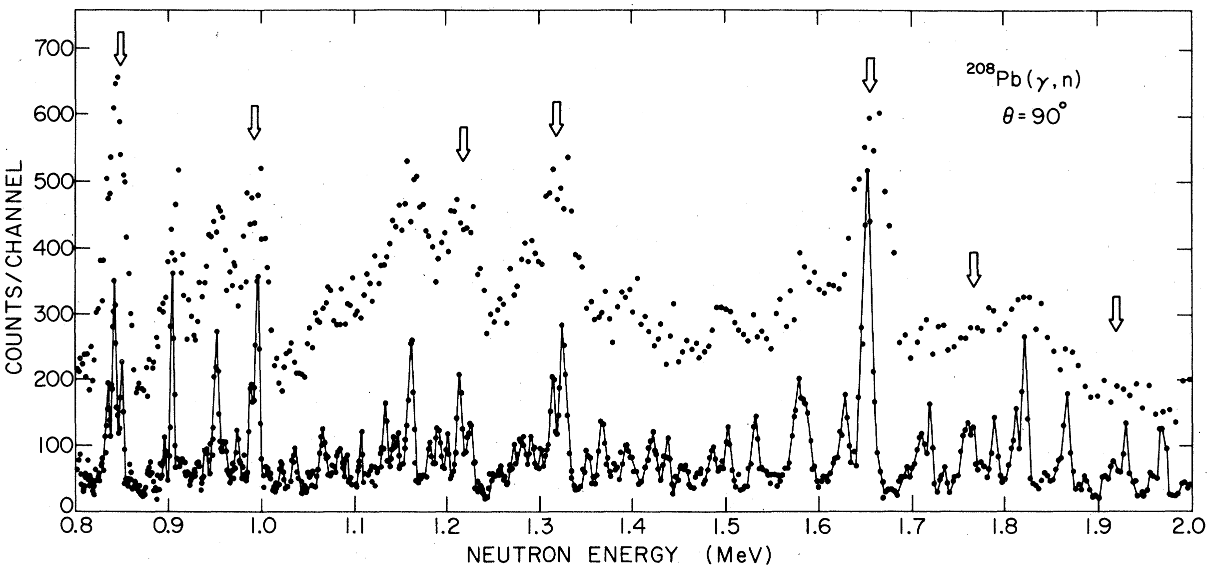

FIG. 10. The high-resolution photoneutron spectrum above 8 MeV. The arrows indicate those regions where significant nonzero (γ, n) polarizations were observed. The uppermost points represent the spectra for the polarization measurement and are compared with the high-resolution spectrum.

the photon, at both in-plane and out-of-plane, was observed in coincidence with the inelastically scattered particle. With this method the resonances at 6.72 and 7.08 MeV were assigned as 1^- resonances and the 7.061-MeV resonance was tentatively assigned as an $M1$ excitation. However, polarized bremsstrahlung studies[20] indicate that the 7.068-MeV resonance is indeed an $E1$ excitation. The only unchallenged $M1$ excitation below the photoneutron threshold is that discovered by Moreh *et al.*[21] This resonance occurs at 7.279 MeV and has a ground-state radiative width of approximately 0.8 eV. The unchallenged $M1$ excitations in ^{208}Pb below 8.4 MeV are summarized in Table VI.

V. $E1$ EXCITATIONS

A. *s-d*-wave admixtures

The photoneutron polarization data not only proved that the 180- and 254-keV resonances were $E1$ excitations but also indicated that these two resonances had a large d-wave component in the neutron decay. For these $E1$ resonances for which we have both photoneutron angular-distribution and polarization data, we have deduced the values of the s-d-wave admixture. Since an $E1$ resonance can decay by s- or d-wave neutrons to the ground state, only two parameters are necessary to describe the photoneutron cross section and polarization. These are the ratio η between the d- and s-wave amplitudes and the difference Δ_{ds} between the nonresonant phase shifts. The expressions for the photoneutron polarization and angular-distribution ratio can be determined from Eq. (1):

$$p(\theta) = 2(dp/d\Omega)/\sigma(\theta)$$

$$= \frac{-1.067\eta \sin\Delta_{ds} \sin 2\theta}{1+\eta^2+\frac{1}{2}(2^{3/2}\eta\cos\Delta_{ds}-\eta^2)P_2(\cos\theta)}$$

and

$$R \equiv \sigma(90°)/\sigma(135°)$$

$$=(8+10\eta^2-4\cdot 2^{1/2}\eta\cos\Delta_{ds})/(8+7\eta^2+2^{3/2}\eta\cos\Delta_{ds}),$$

where

$$\eta \equiv a_d/a_s = \pm(\Gamma_d/\Gamma_s)^{1/2}.$$

Here the Γ_l are the partial neutron widths.

Since only the photon and neutron channels are open below an excitation energy of 8 MeV, one can assume, to a first approximation, that the nonresonant phase difference can be given by the hard-sphere phase difference for neutron scattering. The radius of the hard sphere was adjusted to give the observed value of the off-resonance neutron total cross section[4] near the 180-keV resonance. A good value of this radius was found to be given by

$$a = 1.4(A^{1/3}+1)\ \text{fm} = 9.68\ \text{fm}.$$

The quantity η was then adjusted to reproduce the measured angular-distribution ratios and the polarizations at 135°. Little weight was given to the observed polarization values since these measurements were performed with less energy resolution than the angular distributions and since the effects of multiple neutron scattering on the analyzing

TABLE VII. s-d-wave admixtures for $E1$ excitations in ^{208}Pb.

E_n (keV)	Δ_{ds} (deg)	$\eta=(\Gamma_d/\Gamma_s)^{1/2}$	γ_d/γ_s	$\lvert\eta\rvert$ (Ref. 42)	$R_{\rm cal}$	$p(135°)_{\rm cal}$	$R_{\rm obs}$
179	50.0	$0.7\ ^{+0.3}_{-0.2}$	$3.0\ ^{+1.3}_{-0.9}$	0.60	1.52	0.45	1.51 ± 0.15
253.7	60.0	$-1.3\ \pm0.4$	$-4.2\ \pm1.3$	0.81	0.98	-0.44	0.98 ± 0.10
313.7	66.0	0.28 ± 0.08	0.78 ± 0.22	0.15	1.15	0.26	1.15 ± 0.05
537	83.0	$0.8\ ^{+0.3}_{-0.2}$	$1.6\ ^{+0.6}_{-0.2}$		1.23	0.56	1.23 ± 0.06
600	86.4	$3.3\ \pm1$	$6.1\ \pm1.8$	2.96	1.37	0.37	1.46 ± 0.04
610	87.0	4.43 ± 1.5	$8.1\ \pm2.7$	large	1.52	0.21	1.57 ± 0.08
647	88.9	$0.9\ \pm0.3$	$2.8\ \pm0.9$		1.19	0.56	1.20 ± 0.06
731	92.8	$1.9\ ^{+2.0}_{-0.9}$	$5.3\ ^{+5.5}_{-2.6}$		1.30	0.48	1.29 ± 0.13

power of the Mg target were difficult to assess. More importantly, the polarization values were valuable for establishing the signs and lower limits on the magnitudes of η.

The deduced values of η and Δ_{ds} are summarized in Table VII. In addition, the calculated values of the angular-distribution ratio and polarization are given in the table. In order to relate the present results to theoretical amplitudes for the s- and d-wave components of the resonances, the neutron reduced widths were computed. It was assumed that these $E1$ excitations, observed in the high-resolution photoneutron work, were predominantly single levels. Then the reduced widths γ_l^2 can be computed from the expression

$$\gamma_l^2=\Gamma_l/2P_l(ka),$$

where P_l is the penetration factor and k is the neutron wave number. The ratios of γ_d/γ_s are also shown in Table VII. The values of η are compared with those of Horen *et al.*[42] in the table. The present results are in reasonable agreement with those of Ref. 42. It is clear that the d-wave admixtures can be large even for resonances as low in energy as the 179-keV resonance. The large d-wave admixtures give rise to large angular-distribution ratios in this energy range. It is these large values of the angular-distribution ratios that created confusion in the parity assignments of the early photoneutron measurements.

One might expect the 1^- resonances in ^{208}Pb to decay predominantly by d wave on the basis of the schematic model of Harvey and Khanna.[29] If we assume that the 1^- resonances have the configuration in the exit neutron channel

$$|1^-\rangle=\gamma_s|3p_{1/2}{}^{-1}\otimes 4s_{1/2}\rangle+\gamma_d|3p_{1/2}{}^{-1}\otimes 3d_{3/2}\rangle\ ,$$

then the ratios of the amplitudes $\gamma_d{}^2/\gamma_s{}^2$ can be extracted from the Harvey-Khanna wave functions. The predicted ratios are extremely large throughout the entire energy range in ^{208}Pb. Although one cannot rely on the details of this calculation, it suggests that the large d-wave component in 1^- is due to the proximity of the $3d_{3/2}$ shell model state.

B. $E1$ radiative widths

Most of the observed strength between threshold and 1000 keV was discovered, using the threshold photoneutron polarization method, to be $E1$ in nature. In fact, all of the 1^- resonances, except for the 40.7- and 610-keV levels, in Table II were assigned with the polarization method. The total known $E1$ strength in this energy region was found to be

$$\sum\Gamma_{\gamma 0}(E1)=72.4\ \text{eV}\ .$$

The amount of assigned $M1$ strength is $\sum\Gamma_{\gamma 0}(M1)=7.1$ eV and the $E2$ strength is $\sum\Gamma_{\gamma 0}(E2)=0.78$ eV from Table II. If we assume that the unassigned strength is dipole in nature, then the total amount of unassigned strength is 23.2 eV. Thus, the total possible amount of $E1$ strength in this energy region is 95.6 eV. The limits of the reduced $E1$ transition probability are given by

$$\bar{B}^{\downarrow}_{E1}=0.952\sum\Gamma_{\gamma 0}(E1)/(\Delta E E_\gamma{}^3)$$
$$=\begin{cases}0.14\,e^2\,\text{fm}^2/\text{MeV} & \text{minimum},\\ 0.17\,e^2\,\text{fm}^2/\text{MeV} & \text{maximum},\end{cases}$$

where ΔE and E_γ are the energy interval and the photon energy, respectively, in MeV. The Axel estimate[43] is given by the expression

$$\bar{B}^{\downarrow}_{\rm Axel}=5.8\times10^{-9}E_\gamma{}^2A^{8/3}\left(\frac{\Gamma}{5\ \text{MeV}}\right)e^2\,\text{fm}^2/\text{MeV}\ , \tag{4}$$

where Γ for the Axel estimate is taken to be 5

MeV. The value of the Axel estimate for this region of ^{208}Pb is given by $\overline{B}^{\downarrow}_{\mathrm{Axel}} = 0.56\, e^2\, \mathrm{fm}^2/\mathrm{MeV}$. The observed average $E1$ photon width is $\frac{1}{3}$ to $\frac{1}{4}$ of this value. However, this is consistent with other observations which indicate that the Axel value tends to overestimate the reduced $E1$ width by an approximate factor of 2 to 4 in nuclei with $A \gtrsim 100$. If the observed width $\Gamma = 3.6$ MeV of the giant dipole resonance in ^{208}Pb is used in expression (4), then the estimate of $\overline{B}^{\downarrow}_{E1}$ becomes $0.40\, e^2\, \mathrm{fm}^2/\mathrm{MeV}$. This value is also more than a factor of 2 greater than the observation.

VI. CONCLUSIONS

The photoneutron polarization experiments and the high-resolution photoneutron observations show that there are no large $M1$ excitations between threshold and 8.4 MeV. Inelastic hadron scattering and polarized photon scattering experiments indicate that there are no large $M1$ excitations below threshold. These findings are in disagreement with all previous theories with the exception of the new development of Brown and Speth. In the Brown-Speth theory, the collective $M1$ resonance is predicted to occur near 10 MeV. A relatively small concentration of $M1$ resonances with approximately 14% of the $M1$ sum rule was reported to occur at 7.5 MeV. From the viewpoint of Brown and Speth, this may well be the isoscalar component of the giant $M1$ resonance. It has also been speculated that the giant $M1$ resonance may be strongly quenched in ^{208}Pb. Consequently, this may be all of the $M1$ strength in ^{208}Pb.

The d-wave neutron decay channel of $E1$ excitations in ^{208}Pb was found to be enhanced for many resonances. This enhancement may be due to the proximity of the $3d_{3/2}$ shell in ^{208}Pb. The amount of $E1$ strength near threshold in ^{208}Pb was found to be lower than the Axel estimate as expected.

We wish to thank G. T. Garvey, J. P. Schiffer, G. E. Brown, and T. S. H. Lee for discussions of the problem of collective magnetic dipole resonances in ^{208}Pb. We thank J. E. Monahan for useful discussions of the R-matrix theory. Finally, we thank G. Mavrogenes, D. Ficht, and L. Rawson for providing the best performance from the electron accelerator. This work was performed under the auspices of the U.S. Department of Energy.

---

*Present address: Department of Physics, University of Illinois at Urbana—Champaign, Urbana, Illinois.

[1]C. D. Bowman, R. J. Baglan, B. L. Berman, and T. W. Phillips, Phys. Rev. Lett. 25, 1302 (1970).

[2]M. Mizumoto, Y. Nakajima, R. Bergère, and T. Faketa, Japan Atomic Energy Research Institute Report No. JAERI-M 4520, 1971 (unpublished).

[3]R. E. Toohey and H. E. Jackson, Phys. Rev. C 6, 1440 (1972).

[4]J. A. Harvey, in Proceedings of the Second International School of Neutron Physics (Alushto), edited by Yn. Popov (Joint Institute of Nuclear Research, Dubna, 1974), p. 157.

[5]L. C. Haacke and K. G. McNeill, Can. J. Phys. 53, 1422 (1975).

[6]R. J. Holt and H. E. Jackson, Phys. Rev. Lett. 36, 244 (1976).

[7]R. J. Holt, R. M. Laszewski, and H. E. Jackson, Phys. Rev. C 15, 827 (1977).

[8]R. M. Laszewski, R. J. Holt, and H. E. Jackson, Phys. Rev. Lett. 38, 813 (1977).

[9]D. J. Horen, J. A. Harvey, and N. W. Hill, Phys. Rev. Lett. 38, 1344 (1977).

[10]S. Raman, M. Mizumoto, and R. L. Macklin, Phys. Rev. Lett. 39, 598 (1977).

[11]D. J. Horen, G. F. Auchampaugh, and J. A. Harvey, Phys. Lett. 79B, 39 (1978).

[12]W. Knüpfer, R. Frey, A. Friebel, W. Mettner, D. Meuer, A. Richter, E. Spamer, and O. Titze, Phys. Lett. 77B, 367 (1978).

[13]C. P. Swann, Phys. Rev. Lett. 32, 1449 (1974).

[14]R. M. Del Vecchio, S. J. Freedman, G. T. Garvey, and M. A. Oothoudt, Phys. Rev. Lett. 34, 1296 (1974).

[15]R. M. Del Vecchio, S. J. Freedman, G. T. Garvey, and M. A. Oothoudt, Phys. Rev. C 13, 2089 (1976).

[16]C. P. Swann, Phys. Rev. C 16, 2426 (1977).

[17]W. T. Wagner, G. M. Crawley, G. R. Hammerstein, and H. McManus, Phys. Rev. C 12, 757 (1975).

[18]F. E. Cecil, G. T. Garvey, and W. J. Braithwaite, Nucl. Phys. A232, 22 (1974).

[19]S. J. Freeman, C. A. Gagliardi, G. T. Garvey, M. A. Oothoudt, and B. Svetitsky, Phys. Rev. Lett. 37, 1606 (1976).

[20]A. M. Nathan, R. Starr, R. M. Laszewski, and P. A. Axel, Phys. Rev. Lett. 42, 221 (1979).

[21]R. Moreh, S. Shlomo, and A. Wolf, Phys. Rev. C 2, 1144 (1970).

[22]J. D. Vergados, Phys. Lett. 36B, 12 (1971).

[23]T. S. H. Lee and S. Pittel, Phys. Rev. C 11, 607 (1974).

[24]P. Ring and J. Speth, Phys. Lett. 44B, 477 (1973); Nucl. Phys. A235, 315 (1974).

[25]A. Bohr and B. Mottelson, *Nuclear Structure* (Addison-Wesley, Reading, Massachusetts, 1975), Vol. II, p. 638.

[26]J. S. Dehesa, J. Speth, and A. Faessler, Phys. Rev. Lett. 38, 208 (1977).

[27]M. R. Anastasio and G. E. Brown, Nucl. Phys. A285, 516 (1977).

[28]G. E. Brown and J. Speth, in Proceedings of the Third International Symposium on Neutron Capture Gamma-Ray Spectroscopy and Related Topics, Brookhaven, 1978 (unpublished).

[29]M. Harvey and F. C. Khanna, Nucl. Phys. A221, 77 (1974).

[30]G. S. Mavrogenes, C. Jonah, K. H. Schmidt, S. Gordon, G. R. Tripp, and L. W. Coleman, Rev. Sci. In-

strum. 47, 187 (1976).

[31]A. Horsley, Nucl. Data A4, 321 (1968).

[32]L. Hulthén and B. C. H. Nagel, Phys. Rev. 90, 62 (1952).

[33]S. Raman (private communication).

[34]B. J. Allen and R. L. Macklin, in *Proceedings of the Third Conference on Neutron Cross Sections and Technology, Knoxville, Tennessee*, CONF-71031, 764 (1971) (issued by AEC/OTIE, available NTIS).

[35]S. Raman, in Proceedings of the Third International Symposium on Neutron Capture Gamma-Ray Spectroscopy and Related Topics, Brookhaven, 1978 (unpublished).

[36]S. Raman, M. Mizumoto, G. G. Slaughter, and R. L. Macklin, Phys. Rev. Lett. 40, 1306 (1978).

[37]R. J. Holt, J. R. Specht, H. E. Jackson, and R. M. Laszewski, Nucl. Instrum. Meth. 141, 125 (1977).

[38]J. E. Monahan, R. J. Holt, and R. M. Laszewski (unpublished).

[39]R. J. Holt, R. M. Laszewski, and H. E. Jackson, in *Proceedings of the International Conference on the Interactions of Neutrons with Nuclei, Lowell, Massachusetts, 1976*, edited by E. Sheldon (Technical Information Center, D.O.E., Wasington D.C., 1976), p. 1278.

[40]A. Arima and H. Horie, Prog. Theor. Phys. 12, 623 (1954).

[41]A. Schwierczinski, R. Frey, A. Richter, E. Spamer, H. Theissen, O. Titze, Th. Walcher, S. Krewald, and R. Rosenfelder, Phys. Rev. Lett. 35, 1244 (1975).

[42]D. J. Horen, J. A. Harvey, and N. W. Hill, Phys. Lett. 67B, 268 (1977).

[43]P. Axel, Phys. Rev. 126, 671 (1962).